Calculation of Power Losses in Litz Wire Systems by Coupling FEM and PEEC Method

Andreas Roßkopf, Eberhard Bär, Christopher Joffe, and Clemens Bonse

***Abstract*—The frequency-dependent resistance of inductive components with high-frequency litz wires is essential for the design of power electronic systems. A novel simulation approach is demonstrated, which combines the specific benefits of two numerical methods: The magnetic field distribution is calculated by standard finite-element method tools for complex 3-D geometries based on a solid conductor. The resulting magnetic field on cut sections of the conductor is used as boundary condition for the partial element equivalent circuit method. Based on the coupling of these methods, power losses on litz wire level have been calculated taking different bundle structures and pitch lengths into account. The work flow has been automatized and enables simulations of litz wire systems with hundreds of strands. For different simulation setups, the simulations have been verified by comparison to measurements up to 500 kHz. The average deviation is less than 5% in the relevant frequency range.**

***Index Terms*—Finite-element method (FEM), litz wire, partial element equivalent circuit (PEEC), power losses, proximity effect, simulation, skin effect.**

I. Introduction

In the domain of power electronic systems, prototyping and experiments are time intensive and very costly. The knowledge of parameters such as resistance, inductance, or magnetic field distribution is essential for the design and development process. In the last decades, empirical formulas and analytical approaches are more and more replaced by numerical simulations.

The best-known numerical approach is the finite-element method (FEM) which is established in all engineering domains, such as structural mechanics [1], fluid dynamics [2], or electromagnetics [3]. From the mathematical point of view, the FEM and also the finite differential method are based on the differential equation method. In contrast, the boundary element method (BEM), method of moments [4], and the partial element equivalent circuit (PEEC) [5] are based on the integral formulation. A review on common numerical methods for modeling of induction and electromagnetic systems has been published [6]. In the last years, also approaches using coupling of FEM and BEM have been presented for some specific electromagnetic problems in 2-D [7] and 3-D [8]. Also acceleration techniques like the multipole approach enable calculations of real systems such as shielded induction heaters [9].

Due to high research efforts on numerical algorithms and the increasing computational resources, common electromagnetic simulation software is sufficiently mature for most applications. However, in applications using litz wires, the multiscale structure of these systems results in large differences between measurements and simulations. Research on this topic is highly relevant for the design of all kinds of inductive components, in particular in the domain of inductive power transfer (IPT). The frequency-dependent resistance strongly depends on the winding structure of the litz wire conductor and the ferrite geometry [10]. Different approaches based on accurate measurements of litz wires [11], homogenization of the complex structure [12], [13], [14] or reduction to rotationally symmetric systems [15] are state of the art.

In the following, a novel approach for the simulation of litz wire systems is presented. The work flow is based on the $SlicerPro$ approach introduced in [16] in which the simulation process is splitted. On one hand, the field simulation (with FEM) of the entire system with a solid conductor is carried out. On the other hand, the loss calculation of the litz wire with the structure in detail employs the PEEC method. This work flow combines the specific benefits of both methods stemming from different approaches in the formulation of Maxwell's equations in the solver. Although methods using differential (FEM) or integral (PEEC) formulations solve the same physical system, the solution variables differ and so does the effort for calculations [17].

The basic theory of FEM and PEEC is well known and documented in [18], [19], and [20] and therefore only sketched in Section II. Section III describes the new enhanced simulation approach with focus on the interface of the different numerical methods and the used quality standards. In Section IV, this approach is benchmarked by comparison with measurements for a real coil used for IPT systems [10] with different ferrite geometries. Finally, the conclusions provide an outlook on further improvements of the method and requirements on litz wires and measurement techniques.

II. Theory of FEM and PEEC

The physical basis of electromagnetic phenomena is described by Maxwell's equations. These equations are a coupled system of linear partial differential equations of the electromagnetic fields ($\vec{E}, \vec{H}$), the current and charge density ($\vec{J}, \rho$), and

Manuscript received June 5, 2015; revised August 14, 2015 and September 29, 2015; accepted November 2, 2015. Date of publication November 11, 2015; date of current version March 25, 2016. This work was supported as part of the Energie Campus Nürnberg (EnCN), financed by the State of Bavaria as part of the program Bavaria on the move. This work was also supported by the Bavarian Ministry of Economic Affairs and Media, Energy and Technology as a part of the Bavarian project "Leistungszentrum Elektroniksysteme" (LZE). Recommended for publication by Associate Editor C. R. Sullivan.

The authors are with the Fraunhofer Institute for Integrated Systems and Device Technology, 91058 Erlangen, Germany (e-mail: andreas.rosskopf@iisb.fraunhofer.de; eberhard.baer@iisb.fraunhofer.de; christopher.joffe@iisb.fraunhofer.de; clemens.bonse@iisb.fraunhofer.de).

Color versions of one or more of the figures in this paper are available online at http://ieeexplore.ieee.org.

Digital Object Identifier 10.1109/TPEL.2015.2499793

TABLE I
MAXWELL'S EQUATIONS IN DIFFERENTIAL AND INTEGRAL FORMULATION

Differential formulation	Integral formulation	
$\nabla \times \vec{H} = \vec{J} + \frac{\partial \vec{D}}{\partial t}$	$\oint_L \vec{H} \cdot d\vec{l} = \int_A \left(\vec{J} + \frac{\partial \vec{D}}{\partial t} \right) \cdot d\vec{A}$	(1)
$\nabla \times \vec{E} = -\frac{\partial \vec{B}}{\partial t}$	$\oint_L \vec{E} \cdot d\vec{l} = -\int_A \left(\frac{\partial \vec{B}}{\partial t} \right) \cdot d\vec{A}$	(2)
$\nabla \cdot \vec{D} = \rho$	$\oint_A \vec{D} \cdot d\vec{A} = \int_v \rho dv$	(3)
$\nabla \cdot \vec{B} = 0$	$\oint_A \vec{B} \cdot d\vec{A} = 0$	(4)
	and additionally	
$\vec{D} = \epsilon \vec{E}$	$\vec{B} = \mu \vec{H}$ $\quad \vec{J} = \sigma \vec{E}$	(5)

the material properties (ϵ, μ). There are two common formulations which are shown in Table I with standard notation for all parameters and properties [21].

The FEM approach bases on the differential form of Maxwell's equations. Initially, the entire simulation domain—including air—is divided in subdomains (i.e., triangles in 2-D or tetraeders in 3-D). Discrete shape functions are used for a local approximation of the continuous differential operator on all elements. Recombining these local functions to a global system of equations results in a large, but sparse system of equations (with nonzero entries corresponding to adjacent elements). This matrix represents the entire simulation domain which is solved under the constraints imposed by the boundary conditions [19], [22]. Common FEM programs have highly accurate approaches considering effects of materials with electric and magnetic permeability. Moreover, models with (partial) symmetry can be reduced by appropriate boundary conditions and calculation efforts can be reduced by solvers specialized for partial physical problems (i.e., electrostatic, eddy current) instead of a full-wave simulation. Based on the differential formulation of Maxwell's equations, the solution variables are field values—integral values like resistances or conductivities—need additional postprocessing.

The pros and cons about the FEM can be summed up as follows.

Pros:

1) tight integration in common development processes and simulation work flows;
2) calculation of the electromagnetic field distribution possible even for materials with inhomogeneous electric or magnetic permeability, including the effects of hysteresis (i.e., ferrite).

Cons:

1) time-intensive meshing process (entire domain, including air) and huge amount of elements can lead to a prohibitively large linear system of equations in case of complex structures;
2) calculation of integral values such as resistance and inductance needs additional efforts.

A very convenient numerical approach in the domain of coil simulation is the PEEC method [23]. In contrast to the FEM, the PEEC method uses the integral formulation of Maxwell's equations [24], [25], [5]. In this numeric approach, free space does not need to be resolved—only electrically conductive parts are used in a volumetric representation. At the beginning, the simulation domain is subdivided in partial elements which are considered as parts of an *LRC* circuit. The total electric field $\vec{E}$ at an observation point $\vec{r}$ in the frequency domain ω is given by

$$\vec{E}(\vec{r}, \omega) = -j\omega \vec{A}(\vec{r}, \omega) - \nabla \phi(\vec{r}, \omega) \tag{6}$$

based on (1) and (2).

Instead of the differential operators, Green's integral function G is used to calculate the magnetic vector potential $\vec{A}$ and the electric scalar potential ϕ. Therefore, (6) is restated as

$$\underbrace{\vec{E}(\vec{r}, \omega)}_{\alpha} = \underbrace{-j\omega\mu \int_{v'} G(\vec{r}, \vec{r}') \vec{J}(\vec{r}', \omega) \, dv'}_{\beta} - \underbrace{\frac{\nabla}{\epsilon} \int_{v'} G\left(\vec{r}, \vec{r}'\right) q(\vec{r}', \omega) \, dv'}_{\gamma}. \tag{7}$$

The value of the current density $(\vec{J})$ is stored in the volume v' of each conductor cell, while the surfaces account for the charges (q).

In the simulation of litz wire systems, the capacitive displacement currents between strands and charge accumulation are both second-order effects [26]. Therefore, the γ term in (7) vanishes. The total electric field $\vec{E}$ is only dependent on the magnetic vector potential and, therefore, the current density $\vec{J}$ (β term).

In the simulation, the conductor under study is approximated as a set of piecewise-straight parts. The volume of each straight set is discretized into parallel filaments. By the partial inductance approach [23], the relation between currents and voltages in the filaments can be written as

$$V_b = ZI_b = (R + j\omega L) I_b. \tag{8}$$

This system of equations represents an equivalent electric circuit with n branches, the branch voltage vector $V_b = [V_1, V_2, V_3, \ldots, V_n]^T$ (calculated by the α term [23]), and branch currents $I_b = [I_1, I_2, I_3, \ldots \ , I_n]^T$. The impedance matrix Z is the summation of the diagonal resistance matrix R and dense inductance matrix L. According to Kirchoff's voltage and current laws [27], the mesh-analysis matrix M is introduced by

$$V_s = MV_b \tag{9}$$

and

$$M^T I_m = I_b \tag{10}$$

with the vector of the source branch voltages V_s and the vector of the mesh currents I_m.

Combining (8) with (9) and (10) yields

$$MZM^T I_m = V_s \tag{11}$$

where V_s is always zero except those rows corresponding to terminal voltage excitations. Based on this equation, the terminal

TABLE II
COMPARISON OF PEEC AND FEM FOR A 19×0.25 MM LITZ WIRE OF 30 MM IN LENGTH (SMALL SAMPLE ON THE LEFT SIDE)

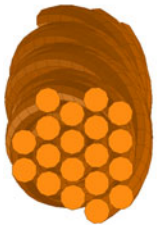

	Elements	RAM	CPU time
FEM	860 k	42.3 GB	5080 sec
PEEC	119 k	1.5 GB	578 sec

behavior of the entire system can be calculated, which also yields the port admittance matrix $inv(MZM^T)$. In common implementations, the system of (11) is solved by iterative algorithms like GMRES or PCG, accelerated by fast matrix-vector approaches such as the fast multipole method [23] or pFFT [26].

In conclusion, advantages and disadvantages can be summarized as follows.

Advantages:

1) time and frequency sweeps can be calculated very efficiently with reduced complexity;
2) the simulation is reduced according to the geometry (limitation to conductive parts) and the electrical complexity (simplifications on circuit level).

Disadvantages:

1) the variety of applications of the PEEC method is limited and focused on circuits and corresponding components. Sophisticated implementations are available for specialized problems [28], whereas rigors EM solver allow the treatment of arbitrary geometries;
2) the calculation of the field and current density distributions requires additional postprocessing.

Well-known implementations, which showed the benefit of the PEEC method 20 years ago, are the extraction programs FASTCAP [29] and FASTHENRY [23], [30]. In the last few years, these approaches where enhanced and adapted to high-performance computers, resulting in tools specialized on the calculation of power losses in litz wires [31], [32]. All these approaches concern pieces of several centimeter of litz wire conductors (i.e., one pitch length of 30 mm) but not an entire power electronic system.

Compared to the FEM, these PEEC-based simulations achieve a significant reduction of computational efforts. The FEM simulation of one pitch length (30 mm) with 19 strands requires approximately 42-GB memory, while the same structure needs 1.5 GB in the PEEC method (see Table II). Due to the limitation to conductive parts, the PEEC method requires less elements (factor 7) than the FEM. Moreover, the large difference in memory (factor 28) also results from the fact, that in elements of the PEEC method only circuit variables are stored while in the FEM memory is required for all electromagnetic field variables [17] (including the ones needed for the postprocessing). The CPU time for the calculation of the power losses for a defined frequency and external magnetic field value shows the same trend: While the PEEC method requires 578 s, the FEM simulation needs eight times longer.

III. SIMULATION APPROACH FOR LITZ WIRE SYSTEMS

In most simulations of winding losses in litz wire systems, simplified structures are used or the system is reduced to 2-D [15]. Our new work flow enhances the approach described in [33] by using loss calculations based on the PEEC method on litz wire level. With the help of this coupled method, the resistance of realistic 3-D litz wire structures with different pitch length or bundle levels are evaluated for the entire power electronic system.

In Fig. 1, the new work flow is sketched in a flow chart diagram starting with the CAD import to a standard FEM program. On geometry level, litz wire conductors are simplified to solid conductors with homogenous excitation by a current density. Even though the current density distribution is inhomogeneous in real systems inside the strands, the total current is distributed equally among all strands (stranded option) in the simulation. This assumption may slightly differ from the behavior in real systems due to skin effect on bundle level [34] and the contact [16]. In case of constant material properties in the regarded frequency range, the physical system can be treated by the magnetostatic solver.

Based on the total field distribution calculated with the FEM program ($\vec{H}_{\text{tot}}$), the internal and external magnetic field along the length of the conductor is evaluated on the surface of the solid conductor, which is shown in Fig. 2. The internal magnetic field of a round conductor with radius r is given by

$$H = \frac{I}{2\pi r}. \tag{12}$$

It is tangential to the surface of the conductor and the intensity depends on the current I. Therefore, when averaging $\vec{H}_{\text{tot}}$ over the cut of the conductor surface (see Fig. 2), only $\vec{H}_{\text{ext}}$ remains which is the external magnetic field the conductor is exposed to and which is the quantity needed for the further loss calculations. Due to the symmetry of the conductor, only the magnitude of the external magnetic field (hereinafter referred as H_{ext}) is needed for further loss calculations. Based on several thousand of cuts along the length of the conductor, the spatial external magnetic field distribution is calculated.

The method of extracting H_{ext} is quite costly compared to taking the values at the center of the conductor. As the internal field vanishes at the center, $\vec{H}_{\text{tot}}$ is equal to the external field $\vec{H}_{\text{ext}}$ there. However, the usage of simulation raw data on surface nodes of the geometry as described above yields much higher accuracy compared to interpolated field values in center positions along the conductor.

The coupling interface between FEM and the PEEC or the analytic method is geometrically located at the surface of the conductor. The magnetic field values calculated by the FEM minus the field generated by the conductor itself are used as boundary condition (external magnetic field) for the simulation on litz wire level. Therefore, the specific benefits of the differing

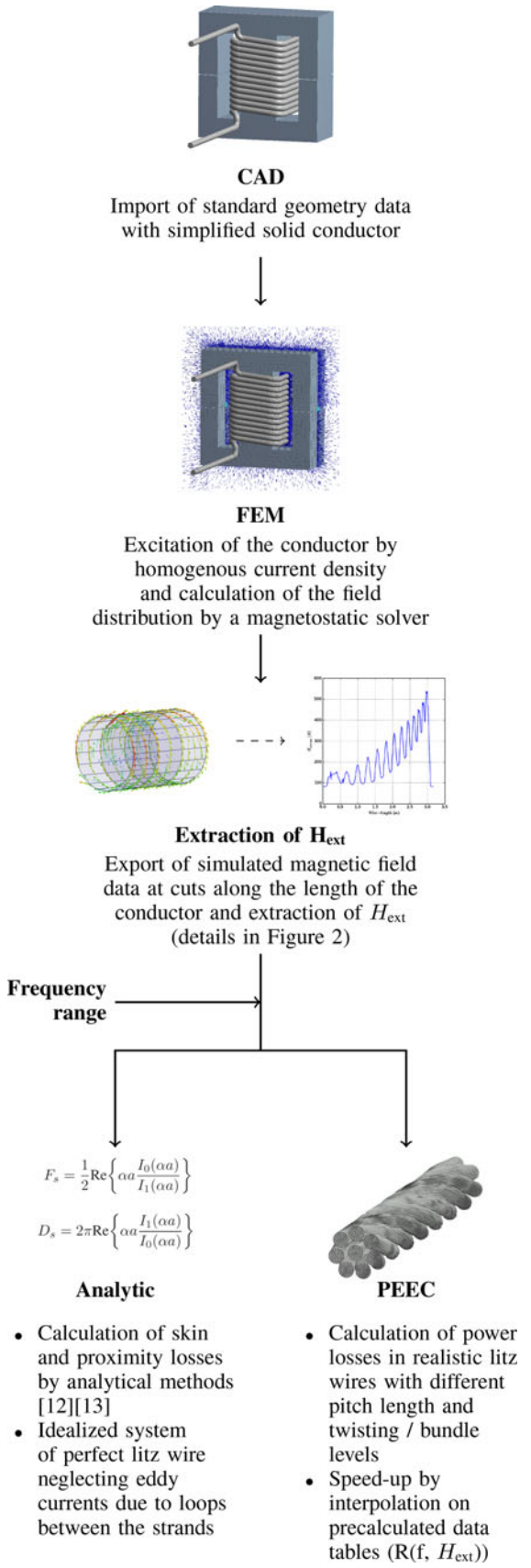

Fig. 1. Schematic work flow of new coupled simulation approach combining FEM with PEEC or analytic methods.

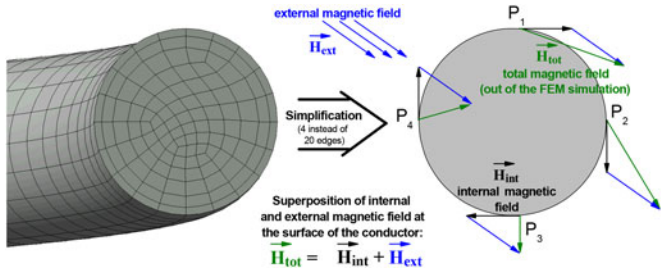

Fig. 2. Left figure shows the mesh of a circular conductor in the FEM simulation. The magnetic field is calculated on all nodes of the circular structure, which is discretized by 20 edges at the conductor surface. On the right side, this structure is simplified and sketched with four points (P_i) on the circle. The entire magnetic field ($\vec{H}_{\mathrm{tot}_i}$) on all nodes is calculated by the FEM and results from the superposition of the internal (black) and external (blue) magnetic field components. By calculating the vectorized average over all $\vec{H}_{\mathrm{tot}_i}$ at the surface, the internal magnetic field components vanish and the averaged external magnetic field remains.

methods are combined to simulate the loss distribution in the entire system: The analytic method enables a very fast and accurate calculation, delivering the theoretical limit of a perfectly twisted conductor, whereas the PEEC method takes into account the realistic 3-D structure of common litz wires.

It has to be noted that the results of the PEEC method are not fed back to the FEM calculations. As the PEEC method assumes equal currents in all strands, deviation from homogeneity would be on strand level. In case of high-frequency litz wires with hundreds of strands, the deviation from homogeneity on strand level has only a very minor influence of bundle level effects [34], [35].

IV. Application on Litz Wire Coil

For many inductive systems, the ferrite structure has significant influence on the coupling and loss behavior. Due to the ferrites, the magnetic field is focused and causes additional local losses, differing depending on the litz wire type and its inner structure.

A. Experimental Setup

In the following, the coil of an IPT system with 12 windings of a 420 × 0.1 mm litz wire such as in Fig. 3(a) is considered. This experimental coil is measured and simulated for four different setups of the ferrite structure [see Fig. 3(b)].

B. Extraction of the External Magnetic Field H_{ext}

The work flow described in Fig. 1 is used for all setups with an excitation current of 1 A homogeneously distributed over the cross section of the solid conductor. The resulting magnetic field distribution on the surface of the conductor [see Fig. 3(c)] shows the superposition of the magnetic field generated by the conductor itself and the external magnetic field. The internal magnetic field at the conductor surface is approximately 108 A/m in case of the chosen conductor of 2.95-mm diameter [see (12)]. In areas with little external fields such as at the top left of the plot, this value is reached, while in the middle of the coil, the magnetic

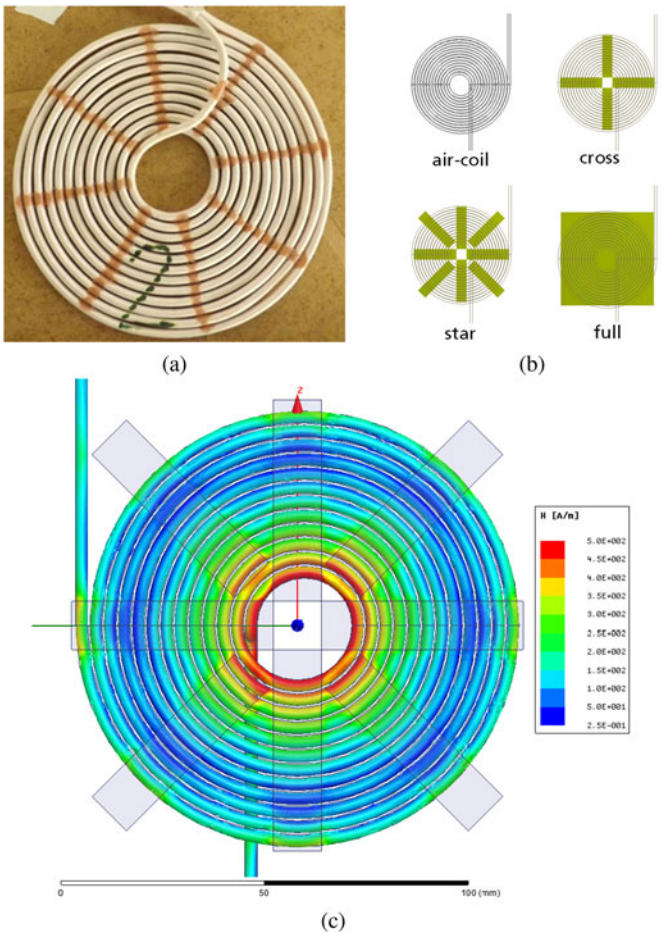

Fig. 3. (a) Experimental coil with 12 windings of a 420 × 0.1 mm litz wire. This coil is used for measurements and simulations as solo coil and with three different ferrite structures shown in (b). In (c), the magnetic field determined by the magnetostatic simulation is plotted on the surface of the coil in case of the star ferrite geometry for a current of 1 A.

field is five times higher as here the external field dominates. In areas near the edges of the underlying ferrite strips, the magnetic field increases by a factor of 2 or even more along a distance of 1 mm.

The extraction of the external magnetic field out of FEM simulation raw data is carried out based on the approach described in Fig. 2. The magnitude of H_{ext} is visualized in Fig. 4 for all four setups of Fig. 3(b). The averaged external magnetic field values are calculated on cuts of 1 mm and plotted along the length of the conductor, starting at the top left of plot 3(c) with nearly no external field. The closer one gets to the middle, the stronger the external magnetic field increases.

Based on this plot, various effects can be investigated:

1) All setups show the same pattern—the inner windings are exposed to the highest fields, while in the outer middle (at the range of 0.5–1.5 m), the external field is the lowest.
2) The periodic structure of peaks for the cross and star geometry shows the ferrite distribution and the conspicuous buckling along the red curve (but also in all others) results from the crossing of the windings to the return conductor [central bottom of Fig. 3(c)].
3) The curve of the air coil defines the minimum over the length, while the full ferrite structure reaches almost throughout the maximum. Nevertheless, especially at the outer winding layers (up to 1 m), the influence of the ferrite strip edges result in peaks with higher magnetic field for the cross and star geometry.

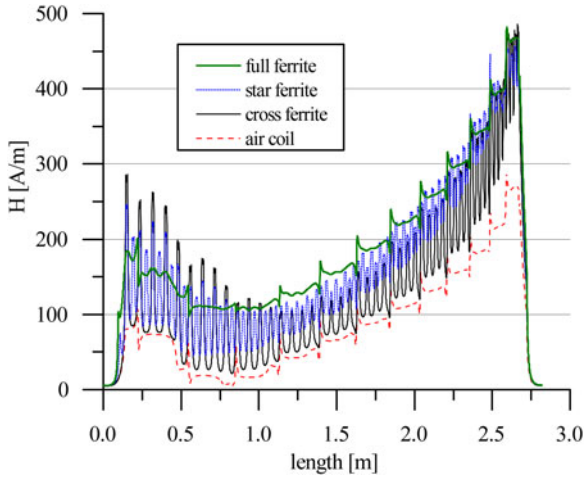

Fig. 4. Averaged external magnetic field H_{ext} for the four different structures of Fig. 3(b) along the length of the conductor. The values are calculated on 3000 cut elements with a length of 1 mm for a current of 1 A.)

C. Loss Calculation With the PEEC Method

The data of the FEM simulation characterize the external magnetic field distribution along the conductor accrued by adjacent windings or ferrite geometries. Based on the spatial resolution along the conductor, the power losses inside the conductor can be calculated depending on the litz wire structure by the PEEC method [36], [26]. In the following, a 420 × 0.1 mm litz wire [37] is used for measurements and simulations of all four ferrite setups. The conductor consists of 14 bundles with 30 strands each and a pitch length of 37 mm.

Using these data for the design of the litz wire in simulations, the resulting diameter of the conductor differs—3.26 mm in the simulation versus 2.95 mm in the experiment. In real litz wires, the package density on strand and bundle level is very tight due to the wrapping. In simulations, the twisting of strands has to be described mathematically—in case of substructures like bundles, this results in a bigger diameter to avoid intersections.

Based on the approximated geometry of the conductor, the power losses P for a wide range of frequencies and external magnetic fields are calculated by the PEEC method. To get an impression for the increase of P with higher frequencies (up to 1 MHz) and external magnetic fields (up to 1000 A/m), a normalized factor $F_P = \frac{P}{P_{\text{DC},0}}$ is introduced. This dimensionless factor is equal to 1 in the dc case without external magnetic field and visualized in Fig. 5 for the relevant ranges.

For low frequencies (up to 10 kHz), P is equal to P_{DC} and the proximity effect has only marginal influence on power losses.

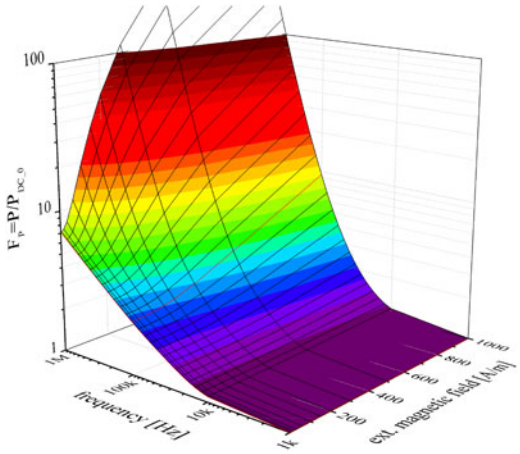

Fig. 5. Influence of frequency and external magnetic field on power losses of a litz wire with 14 bundles with 30 strands. The losses are normalized to the dc case without external magnetic field and for one pitch length (37 mm). The curve for 100 kHz and varying magnetic field is highlighted (red line).

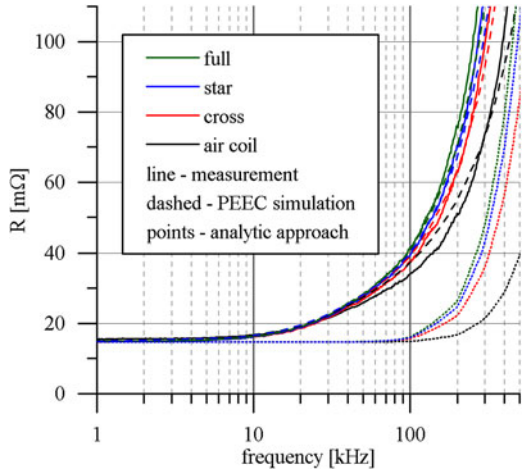

Fig. 6. Measurement and simulation results of the frequency-dependent resistance for four different ferrite setups corresponding to four different colors. The resistance of the system is plotted for frequencies up to 500 kHz for a 420×0.1 mm litz wire. The substructure of the conductor consists of 14 bundles with 30 strands with a pitch length of 37 mm. Moreover, the analytic results for a perfectly twisted conductor of 420 strands is visualized by pointed lines based on simplified 2-D calculations.

For frequencies higher than 10 kHz, the power losses have a polynomial (n between 1.9 and 3.4, depending on the external magnetic field) dependence on the frequency. Interpolations for defined frequency and external magnetic field values have to take this into account.

D. Loss Calculation on System Level

For calculating power losses on system level, the averaged magnetic field along the length of the conductor (see Fig. 4) has to be combined with the loss characteristic of the regarded litz wire (see Fig. 5). However, the length intervals differ: The distance between cuts in Fig. 4 is 1 mm in average, while the PEEC approach uses a pitch length of 37 mm for the power loss calculation. Consequently, when summing up power losses of all cuts, a correction factor ($\frac{L_{\text{cut}}}{L_{\text{pitch}}}$) needs to be applied.

Applying this work flow on the frequency range from 1 kHz to 1 MHz allows us to determine the power losses of the entire system. Based on the excitation current, the initial FEM simulation, the results can be transferred to resistance values according to $\mathrm{P} = \mathrm{I}_{\text{eff}}^2 \cdot \mathrm{R}$. In Fig. 6, these simulation results are compared to measurements with a 4294A Precision Impedance Analyzer of Agilent Technologies. The four different ferrite setups show the expected shape: the higher the ferrite coverage, the higher is the frequency dependent resistance. Measured (solid lines) and simulated (dashed lines) curves have the same shape and especially simulations of setups including ferrites (cross, star, full) very well agree with measurements over the entire frequency range studied. Standard approaches using the analytic methods of [12] and [13] (visualized by pointed lines) show a high deviation to measurements and are therefore inappropriate to depict the system behavior of real litz wires at higher frequencies.

In the relevant frequency range of IPT systems from 50 to 200 kHz, the averaged deviation between the coupled FEM/PEEC simulation and the measurement is less than 5% for all setups studied.

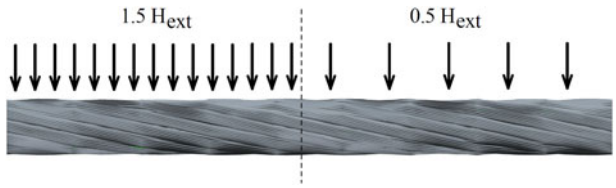

Fig. 7. Section of one pitch length (37 mm) of a litz wire with 420 strands exposed to an inhomogeneous external magnetic field. One half with $1.5 \cdot H_{\text{ext}}$, the other half with $0.5 \cdot H_{\text{ext}}$.

E. Effect of the Field Averaging

One dominating error source is the usage of averaged magnetic field values in each cut. The inhomogeneous field distribution inside the conductor is lumped into an averaged value for the PEEC simulation. By using these averaged values, the precalculated data for a litz wire (visualized in Fig. 5) enable the loss calculation for the entire system, while a spatial variation of the field would require hundreds of individual PEEC simulations. However, for estimating the error resulting from using a single value, analytic formulas [38] for the proximity losses can be used, such as

$$P_{\text{prox}} = \frac{l}{\kappa} H_{\text{ext}}^2 \cdot D_s \tag{13}$$

which shows the quadratic influence of H_{ext} at a given specific conductance κ and proximity factor D_s. For example, a line conductor exposed to an inhomogeneous field (see Fig. 7) of one half with $1.5 \cdot H_{\text{ext}}$ and second half with $0.5 \cdot H_{\text{ext}}$ exhibits in 25% higher proximity losses compared to the case of homogeneous field.

In Fig. 8, the influence of an inhomogeneous magnetic field distribution as specified above is shown for a 420×0.1 mm litz wire (13 bundles with 40 strands) and 100 kHz. It can be seen

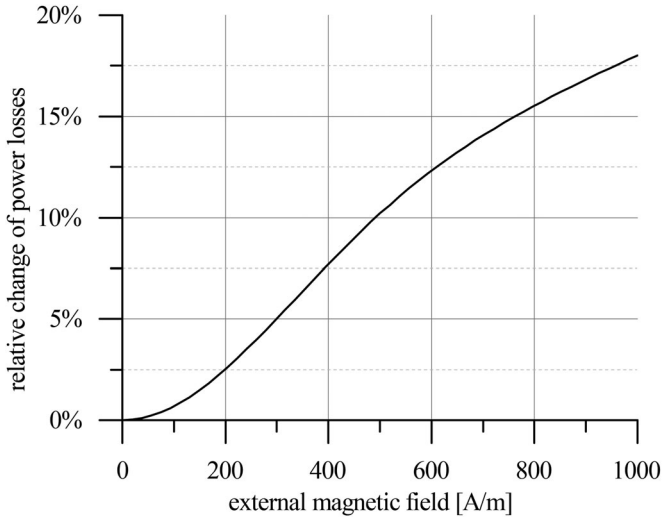

Fig. 8. Increase of the entire power losses (due to skin, internal, and external proximity effect) in percentage for a 420 litz wire (13 bundles with 40 strands) at 100 kHz due to inhomogeneous external magnetic field (like in Fig. 7). The change is taken relative to the case where the conductor is exposed to a homogenous external magnetic field H_{ext}.

that an increasing magnetic field leads to an increasing relative change of power losses. For the typical conditions studied, H_{ext} is in the range up to 500 A/m. Therefore, according to Fig. 8, a relative error up to approximately 10% can be attributed to an inhomogeneous field distribution. In addition, it should be note that these relative changes of power losses depend also on the inner structure of the litz wire.

In conclusion, we consider this effect and the simulation error resulting from the difference in the simulated geometry to the experiment (see above) as the main reasons for the derivation between simulation and measurement.

V. Results and Conclusion

The presented simulation work flow shows new capabilities for the calculation of frequency-dependent resistances in litz wire systems with ferrite materials. It is shown how standard numerical tools can be combined in a work flow to simulate 3-D systems with high complexity thereby enhancing common coupled FEM/BEM approaches. For the first time, complex 3-D geometries with ferrite materials are combined with calculations on litz wire level. This is achieved by performing simulations for complex geometries on system level (with the FEM) combined with modeling of litz wires on substructure level using the PEEC method. Power loss and resistance can be determined over a large range of frequencies. Among others, the method enables one to study the influence of the substructure of the conductor with different pitch lengths on strand and bundle level.

Simulation results show a good agreement with measurements over a wide frequency range for different geometry setups. Using this work flow combined with thermal simulations has the potential to improve the accuracy of simulations used for investigating various inductive coupling systems. To realize simulations with higher accuracy, more data about the inner structure of the litz wires need to be provided (i.e., pitch length on strand level). Moreover, common algorithms for the design of the geometrical structures need to be enhanced to reproduce the very dense package of strands due to the wrapping. In addition, the inhomogeneous external magnetic field distribution needs to be considered in the loss calculation. However, to allow these calculations with reasonable computational effort, major adaptions of the PEEC implementation are required.

References

[1] M. Rodriguez and N. Y. Shammas, "Finite element simulation of thermal fatigue in multilayer structures: Thermal and mechanical approach," *Microelectron. Rel.*, vol. 41, no. 4, pp. 517–523, 2001.
[2] T. E. Tezduyar and A. Sameh, "Parallel finite element computations in fluid mechanics," *Comput. Methods Appl. Mech. Eng.*, vol. 195, no. 13, pp. 1872–1884, 2006.
[3] J. Davies and P. Silvester, "Finite elements in electromagnetics: A jubilee review," *Appl. Comput. Electromagn. Soc. J.*, vol. 9, pp. 10–24, 1994.
[4] M. Costabel and E. Stephan, "A direct boundary integral equation method for transmission problems," *J. Math. Anal. Appl.*, vol. 106, no. 2, pp. 367–413, 1985.
[5] A. E. Ruehli, "Equivalent circuit models for three-dimensional multiconductor systems," *IEEE Trans. Microw. Theory Tech.*, vol. MTT-22, no. 3, pp. 216–221, Mar. 1974.
[6] S. Lupi, F. Dughiero, E. Baake, and J. Lavers, "State of the art of numerical modeling for induction processes," *COMPEL-The Int. J. Comput. Math. Electr. Electron. Eng.*, vol. 27, no. 2, pp. 335–349, 2008.
[7] V. M. Machado, "FEM/BEM hybrid method for magnetic field evaluation due to underground power cables," *IEEE Trans. Magn.*, vol. 46, no. 8, pp. 2876–2879, Aug. 2010.
[8] Z. Liu, Y. Wang, Z. Jia, and Y. Sun, " A novel hybrid FEM-BEM method for 3D eddy current field calculation using current density kj," *Sci. China Series E: Technol. Sci.*, vol. 46, no. 1, pp. 41–48, 2003.
[9] R. Sabariego, P. Sergeant, J. Gyselinck, P. Dular, L. Dupré, and J. Melkebeek, "Fast multipole accelerated finite element-boundary element analysis of shielded induction heaters," *IEEE Trans. Magn.*, vol. 42, no. 4, pp. 1407–1410, Apr. 2006.
[10] C. Joffe, S. Ditze, and A. Rokopf, "A novel positioning tolerant inductive power transfer system," in *Proc. 3rd Int. Electr. Drives Prod. Conf.*, Oct. 2013, pp. 1–7.
[11] H. Rossmanith, M. Döbrönti, M. Albach, and D. Exner, "Measurement and characterization of high frequency losses in nonideal litz wires," *IEEE Trans. Power Electronics*, vol. 26, no. 11, pp. 3386–3394, Nov. 2011.
[12] H. Rossmanith, A. Manfred, P. Janina, and S. Alexander, "Improved characterization of the magnetic properties of hexagonally packed wires," in *Proc. 14th Eur. Conf. Power Electron. Appl.*, Aug. 2011, pp. 1–9.
[13] X. Nan and C. Sullivan, "An equivalent complex permeability model for litz-wire windings," in *Proc. 14th IAS Annu. Meet.. Conf. Rec. Ind. Appl. Conf.*, Oct. 2005, vol. 3, pp. 2229–2235.
[14] D. C. Meeker, "An improved continuum skin and proximity effect model for hexagonally packed wires," *J. Comput. Appl. Math.*, vol. 236, no. 18, pp. 4635–4644, Dec. 2012.
[15] P. Reddy, T. Jahns, and T. Bohn, "Modeling and analysis of proximity losses in high-speed surface permanent magnet machines with concentrated windings," in *Proc. IEEE Energy Convers. Congr. Expo.*, Sep. 2010, pp. 996–1003.
[16] A. Roßkopf, E. Bär, and C. Joffe, "Influence of inner skin- and proximity effects on conduction in litz wires," *IEEE Trans. Power Electronics*, vol. 29, no. 10, pp. 5454–5461, Oct. 2014.
[17] T.-S. Tran, G. Meunier, P. Labie, and J. Aime, "Comparison of FEM-PEEC coupled method and finite-element method," *IEEE Trans. Magn.*, vol. 46, no. 4, pp. 996–999, Apr. 2010.
[18] J. D. Jackson, *Classical Electrodynamics*, 3rd ed. New York, NY, USA: Wiley, 1999.
[19] O. C. Zienkiewicz and R. L. Taylor, *The Finite Element Method Set*, 6th ed. London, U.K.: Butterworth-Heinemann, 2005.
[20] M. N. Sadiku, *Numerical Techniques in Electromagnetics*, 2nd ed. Boca Raton, FL, USA: CRC Press, 2001.
[21] J. Ekman, "Electromagnetic modeling using the partial element equivalent circuit method," Ph.D. dissertation, EISLAB Dept. Comput. Sci. Elect. Eng., Univ. Technol. Luleå, Luleå, Sweden, 2003.

[22] S. Humphries, Jr, *Field Solutions on Computers*. Boca Raton, FL, USA: CRC Press, 1997.
[23] M. Kamon, M. Tsuk, and J. White, "FASTHENRY: A multipole-accelerated 3-D inductance extraction program," *IEEE Trans. Microw. Theory Techn.*, vol. 42, no. 9, pp. 1750–1758, Sep. 1994.
[24] A. E. Ruehli, "Inductance calculations in a complex integrated circuit environment," *IBM J. Res. Dev.*, vol. 16, no. 5, pp. 470–481, Sep. 1972.
[25] A. E. Ruehli and P. A. Brennan, "Efficient capacitance calculations for three-dimensional multiconductor systems," *IEEE Trans. Microw. Theory Techn.*, vol. MTT-21, no. 2, pp. 76–82, Feb. 1973.
[26] R. Zhang, J. White, and J. Kassakian, "Fast simulation of complicated 3-d structures above lossy magnetic media," *IEEE Trans. Magn.*, vol. 50, no. 10, pp. 1–16, Oct. 2014.
[27] R. Unbehauen, *Grundlagen der Elektrotechnik: Allgemeine Grundlagen, Lineare Netzwerke, Stationäres Verhalten* (ser. Springer-Lehrbuch). Berlin, Germany: Springer, 2013.
[28] G. Antonini, J. Delsing, J. Ekman, A. Orlandi, and A. Ruehli, "PEEC development road map 2007," Dept. Elect. Eng., Univ. L'Aquila, L'Aquila, Italy, Tech. Rep., 2009-Q1, 2007.
[29] K. Nabors and J. White, "FastCap: A multipole accelerated 3-D capacitance extraction program," *IEEE Trans. Comput.-Aided Design Integrated Circuits Syst.*, vol. 10, no. 11, pp. 1447–1459, Nov. 1991.
[30] J.-R. Li and M. Kamon, " PEEC model of a Spiral Inductor Generated by Fasthenry," in *Dimension Reduction of Large-Scale Systems* (ser. Lecture Notes in Computational Science and Engineering), vol. 45, P. Benner, D. Sorensen, and V. Mehrmann, Eds. Berlin, Germany: Springer, 2005, pp. 373–377.
[31] C. Sullivan and R. Zhang, "Simplified design method for litz wire," in *Proc. 29th Annu. IEEE Appl. Power Electron. Conf. Expo.*, Mar. 2014, pp. 2667–2674.
[32] J. Acero, I. Lope, J. Burdio, C. Carretero, and R. Alonso, "Loss analysis of multistranded twisted wires by using 3D-FEA simulation," in *Proc. IEEE 15th Workshop Control Model. Power Electron.*, Jun. 2014, pp. 1–6.
[33] A. Roßkopf, C. Joffe, and E. Bär, "Calculation of ohmic losses in litz wires by coupling analytical and numerical methods," in *Proc. 4th Int. Electr. Drives Prod. Conf.*, Sep. 2014, pp. 1–6.
[34] C. R. Sullivan, "Optimal choice for number of strands in a litz-wire transformer winding," *IEEE Trans. Power Electron.*, vol. 14, no. 2, pp. 283–291, Mar. 1999.
[35] M. Albach, "Two-dimensional calculation of winding losses in transformers," in *Proc. IEEE 31st Annu. Power Electroni. Spec. Conf.*, 2000, vol. 3, pp. 1639–1644.
[36] R. Y. Zhang. (2014, Mar.). FastLitz—Realistic litz wire characterization. [Online]. Available: http://web.mit.edu/ryz/www/zip/fastlitzv1a.zip
[37] Rudolf Pack GmbH & Co. Technical Data RUPALIT Litz wire. (2015). [Online]. Available: http://www.pack-feindraehte.de/en/products/litzwire/litzentabelle.pdf
[38] J. Mühlethaler, "Modeling and multi-objective optimization of inductive power components," Ph.D. dissertation, ETH Zürich, Zürich, Switzerland, 2012.

Andreas Roßkopf studied applied mathematics in Erlangen, Germany. He received the Diploma degree in 2008.

He worked for companies in automotive and electrical sector as an CAE Engineer. In 2012, he joined the Fraunhofer Institute for Integrated Systems and Device Technology, Erlangen. His research interests include modeling and simulation of electrical and thermal effects in power electronic systems.

Eberhard Bär received the Diploma degree in physics from the Darmstadt University of Technology, Darmstadt, Germany, in 1992, and the Ph.D. degree in electrical engineering from the University of Erlangen-Nuremberg, Erlangen, Germany, in 1998.

In 1992, he joined the Fraunhofer Institute for Integrated Systems and Device Technology, Erlangen, where he is a Team Leader of the structure simulation group.

Christopher Joffe received the Diploma degree in mechatronics from the Dresden University of Technology, Dresden, Germany, in 2011. He is currently working toward the Ph.D. degree at the Fraunhofer Institute for Integrated Systems and Device Technology, Erlangen, Germany, in the Department of Power Electronic Systems.

His research interests include inductive power transfer systems and resonant converters.

Clemens Bonse received the Bachelor's degree in mechatronics from the University in Erlangen-Nuremberg, Erlangen, Germany, in 2014.

He is currently working at the Fraunhofer Institute for Integrated Systems and Device Technology, Erlangen, in the team of structure simulation.